

# Strongly Correlated Photons in a Two-Dimensional Array of Photonic Crystal Microcavities

Y.C. Neil Na,<sup>1</sup> Shoko Utsunomiya,<sup>2</sup> Lin Tian,<sup>1</sup> and Yoshihisa Yamamoto<sup>1,2</sup>

<sup>1</sup>*E. L. Ginzton Laboratory, Stanford University, Stanford, CA 94305, USA*

<sup>2</sup>*National Institute of Informatics, Hitotsubashi, Chiyoda-ku, Tokyo 101-8430, Japan*

We propose and investigate a practical scheme to observe the photonic quantum phase transition (QPT) from superfluid to Mott-insulator states. The photon hopping energy is controlled by the optical evanescent field coupling between two adjacent photonic crystal microcavities, while the photon-photon interaction energy is provided by the strong coupling between many atoms and single mode cavity. We show that our scheme can be implemented using a two-dimensional array of semiconductor photonic crystal microcavities doped with substitutional donor or acceptor impurities. Such a system is robust against the fluctuation of the number of impurities from one site to another, and requires only a moderate cavity  $Q$  factor when choosing an appropriate cavity photon-bound exciton frequency detuning. We also show that in the large detuning limit, our system acts as coupled cavities with optical Kerr nonlinearity where the conventional Bose-Hubbard model is recovered.

Quantum many-body systems, such as strongly correlated electrons, are generally difficult to understand due to the lack of appropriate theoretical tools. A brute-force matrix diagonalization method is limited by the exponentially growing Hilbert space dimension with the number of particles. A quantum Monte-Carlo simulation method often suffers from the so-called sign problem. An analytical mean-field method provides

good approximate solutions for three-dimensional systems but limited applications for two-dimensional systems. An interesting alternative is to construct a quantum simulator that implements a model Hamiltonian with controllable parameters [1]. One such example was demonstrated using Bose-condensed cold atoms in an optical lattice potential. The superfluid to Mott-insulator QPT predicted by the Bose-Hubbard model was observed by changing the ratio of on-site repulsive interaction to hopping matrix element  $U/t$  [2]. This experiment opened a door for simulating complex many-body systems with more controllable artificial systems [3,4].

Simulating the Bose-Hubbard model using photons has recently attracted an intense interest [5,6,7]. Even though photons do not interact with each other in free space, by confining light inside a small cavity with an active medium, the nonlinear photon-photon interaction can be effectively introduced. A related concept is a photon blockade: an optical analog of single electron Coulomb blockade effect [8,9]. These schemes require an extremely high-Q cavity even though EIT in a four-level atomic ensemble or single-atom cavity QED in the strong coupling regime are employed.

In this letter, we show that an optical quantum simulator for such strongly correlated photonic systems can be constructed using a simpler approach. Our scheme consists of a two-dimensional array of coupled photonic crystal microcavities [10] doped with substitutional donor or acceptor impurities [11,12]. The photons hop from site to site via optical evanescent field coupling and interact with each other through the nonlinearity induced by the many-exciton cavity QED effect. Specific example using GaAs photonic crystal microcavities doped with Si donor impurities is investigated as an experimental system. Setting bulk doping density to  $10^{14} \text{ cm}^{-3}$ , cavity photon-bound exciton frequency

detuning around hundreds of GHz and cavity  $Q$  factor about  $10^4$  to  $10^5$ , the QPT from photonic superfluid to Mott-insulator should be observed. The proposed scheme combines the large oscillator strength and small inhomogeneous linewidth of donor/acceptor-bound excitons embedded in bulk semiconductor matrix [11], and the recent advancement in photonic crystal microcavities with high cavity  $Q$  factor and small mode volume [13]. In particular, we will show that the inevitable impurity number fluctuation at each site does not seriously degrade the system performance and therefore no need to control the number of impurities per cavity precisely one [6,7]. In addition, when using a blue detuning, the increase of exciton fraction of the lower branch of the cavity polaritons decreases the required cavity  $Q$  factor. Finally, in the large detuning limit, our system is described by an effective Hamiltonian, which is equivalent to the conventional Bose-Hubbard model for the photon-like branch of the cavity polaritons.

We start our analysis by considering the optical evanescent field coupling between adjacent microcavities. The tunneling part of the Hamiltonian is given as

$$H_{\text{tunneling}} = -t \sum_{\langle ij \rangle} a_i^\dagger a_j \quad (1)$$

where  $\langle ij \rangle$  indicates that only the nearest neighbor coupling is considered.  $t$  is the tunneling energy determined by the overlapping of the nearest neighbor cavity fields, and  $a_i$  is the annihilation operator of the  $i$ th site cavity mode. To quantitatively estimate the condition of QPT, we perform a mean field analysis by applying the decoupling approximation [7,14] i.e. let  $a_i^\dagger a_j = \langle a_i^\dagger \rangle a_j + a_i^\dagger \langle a_j \rangle - \langle a_i^\dagger \rangle \langle a_j \rangle$  and define a real-valued superfluid parameter  $\psi = \langle a_i \rangle$ . (1) can then be rewritten as

$$H_{\text{tunneling}} = \sum_i H_{\text{tunneling}}^i = \sum_i \{-zt\psi(a_i^\dagger + a_i) + zt\psi^2\} \quad (2)$$

where  $z$  is the number of nearest neighbors. A schematic plot of a two-dimensional array of coupled photonic crystal microcavities is shown in Fig. 1.

Next we consider the free and interacting part of the total Hamiltonian

$$H_{\text{free}} = \sum_i H_{\text{free}}^i = \sum_i \left\{ \omega_e (L_z^i + N_i/2) + \omega_p a_i^\dagger a_i \right\}, \quad (3)$$

$$H_{\text{interacting}} = \sum_i H_{\text{interacting}}^i = \sum_i \left\{ g (L_-^i a_i^\dagger + L_+^i a_i) \right\}. \quad (4)$$

$\omega_e$ ,  $\omega_p$  and  $g$  are the bound exciton transition frequency, cavity photon resonance frequency and exciton-photon coupling constant.  $N_i$  is the number of impurities per cavity.  $L_z$  is the collective angular momentum operator in the  $z$  direction and  $L_\pm$  are the collective creation/annihilation operators. Notice that the lowest eigenenergy is chosen to be zero in writing down (3) and (4). The single site eigenenergy spectrum considering only the free and interacting Hamiltonian is sketched in Fig. 2. In general, the number of eigenstates for each excitation manifold  $n$  is equal to  $n+1$  if  $n \leq N$  and equal to  $N+1$  if  $n > N$ . The ground state (lower branch of the cavity polaritons of  $n=1$  excitation manifold) interaction energy  $U$  can then be identified and is shown in Fig. 2. Notice that in the small detuning limit,  $U$  approaches zero if  $N$  is much larger than  $n$ . In this case, the system behaves linearly because the collective angular momentum operator satisfies a bosonic commutation relation  $[L_+, L_-] \sim N$  [15]. On the other hand, in the large red detuning limit,  $U$  is linearly proportional to  $N$ . Such a trend is originated from the optical Kerr nonlinearity and we will come back to this point later.

Equipped with Hamiltonian (2), (3) and (4), we are now in position to evaluate the QPT condition. We consider only a single site Hamiltonian

$$H^i = H_{\text{tunneling}}^i + H_{\text{free}}^i + H_{\text{interacting}}^i - \mu (L_z^i + N_i/2 + a_i^\dagger a_i) \quad (5)$$

where  $\mu$  is the chemical potential in grand canonical ensemble. Given  $t$  and  $\mu$ , one can calculate the eigenenergies by diagonalizing (5) using bare states as a complete set of basis. The ground state energy can be found by minimizing the lowest eigenenergy with adjusting the superfluid parameter. The accuracy of such calculation depends on how many state vectors are used to span the Hilbert space. The convergence of the eigenenergies is usually a good indication that a large enough basis set is considered. Repeating such procedures, we can generate the phase diagram with reasonable computational resource. In Fig. 3, we plot the superfluid parameter as a function of  $t$  and  $\mu$  given  $N=8$  and  $\Delta=\omega_p-\omega_e=0$ . Unlike the single-atom cavity QED systems [6,7], the Mott lobe sizes in the chemical potential direction are relatively unchanged for low filling factors. The nature of such a photonic QPT is neither purely fermionic nor bosonic, but shares similar features with the Bose-Hubbard model: localization of one additional photon per cavity upon entering the next Mott-insulator regime.

To understand the general behavior of the QPT condition, we plot the required  $t$  for the system to enter the Mott-insulator regime as a function of  $N$  and  $\Delta$ . This is shown in Fig. 4a. The numerical value of  $\omega_e/2\pi$  is chosen as 365.8 THz that corresponds to 820 nm Si donor-bound exciton emission wavelength [11].  $g$  is estimated as 33.2 GHz by calculating the bound exciton oscillator strength using the experimentally measured 1 ns lifetime [11], and a cavity mode volume equal to  $(820/3.25)^3$  nm<sup>3</sup>. 3.25 is the refractive index of GaAs. As previously explained, the system behaves linearly if  $N$  is sufficiently large and hence the  $t$  required for the system to enter the Mott-insulator regime decreases as  $N$  increases. In addition, by having a blue detuning i.e.  $\Delta>0$ , the ground state is of more exciton fraction. Therefore, the tunneling energy provided by optical evanescent

field coupling has to be stronger in order to maintain the QPT condition. Finally, the fluctuation of the number of impurities would not seriously influence the QPT condition. For example, setting the average number of impurities per cavity equal to 9, which corresponds to a bulk doping density about  $5.6 \times 10^{14} \text{ cm}^{-3}$ , the  $t$  required to reach the QPT deviates about 18% from its average value if the number of impurities obeys a Poisson distribution. Such a small distribution of  $t$  can be easily absorbed by the experimental errors and largely reduces the difficulties using single-atom cavity QED system.

The leakage of the cavity photons imposes an important constraint on the required cavity  $Q$  factor. If the photon decay rate in the Mott-insulator regime is faster than the photon tunneling rate, the system never reaches an equilibrium state described by Hamiltonian (5). Suppose the ground state decay rate is slower than the tunneling rate, we arrive at the required cavity  $Q$  factor as

$$Q \geq \frac{|c_p|^2 \omega_p}{|c_p|^2 t - |c_e|^2 \frac{F}{\tau_e}}. \quad (6)$$

$|c_e|^2$  and  $|c_p|^2$  are the exciton and photon fraction of the ground state,  $t$  is the required tunneling energy for the system to enter the Mott-insulator state, and  $\tau_e$  is the bound exciton spontaneous emission lifetime. The Purcell factor  $F$  is due to the inhibition of spontaneous emission in a photonic crystal results from the reduced local optical density of states. We plot the required  $Q$  value in Fig. 4b as a function of  $N$  and  $\Delta$  where  $F=0.2$  is used [16,17]. In general,  $Q$  about  $10^5$  to  $10^6$  is needed to reach the OPT point. However, with a blue detuning, cavity  $Q$  factor is reduced due to the increase of the exciton fraction and the increase of the required  $t$  to reach QPT. This way, in principle, cavity  $Q$  factor

can be relaxed by choosing a sufficiently large blue detuning. For example,  $Q$  is less than  $10^5$  when  $\Delta=8g$  for  $N=8$ .

Up to now, we have shown that the many-exciton cavity QED Hamiltonian (5) generates similar dynamics to the conventional Bose-Hubbard model. In a large red detuning limit, the ground state can be described by an effective Hamiltonian

$$H = \int \frac{1}{2} \varepsilon_o K_C \vec{E}^2 dV + \int \frac{1}{2} \mu_o \vec{H}^2 dV + \int \frac{1}{2} \varepsilon_o \chi_C^{(3)} \vec{E}^4 dV. \quad (7)$$

$E$  and  $H$  are electric and magnetic field operators.  $\varepsilon_o$  and  $\mu_o$  are the free space permittivity and permeability.  $K_C$  is the position dependent dielectric constant of the coupled photonic crystal microcavities and  $\chi_C^{(3)}$  is the position dependent optical Kerr nonlinearity. All of the exciton-photon interaction can be renormalized into the linear and nonlinear dielectric constants by adiabatically eliminating the excitonic degrees of freedom. By substituting the electric and magnetic field operators into (7), which consists of the localized Wannier function based on isolated cavity field, we arrive

$$H = -t \sum_{\langle ij \rangle} a_i^\dagger a_j + \frac{U}{2} \sum_i a_i^\dagger a_i^\dagger a_i a_i \quad (8)$$

where

$$t = -2 \varepsilon_o \int_V K_C(\vec{r}) \vec{\phi}(\vec{r}) \vec{\phi}(\vec{r} - \vec{d}) dV, \quad (9)$$

$$U = 6 \varepsilon_o \int_V \chi_C^{(3)}(\vec{r}) \vec{\phi}^4(\vec{r}) dV. \quad (10)$$

$\phi$  is the cavity mode electric field assumed to be real, and  $d$  is the inter-cavity distance. Arriving at (8), we consider only the nearest neighbor photon hopping and on-site photon-photon interaction using rotating wave approximation. Unlike the system Hamiltonian (5), the effective Hamiltonian (8) is identical to the Bose-Hubbard model.

Operating the system in such a large red detuning limit serves as a potential candidate for implementing a quantum simulator for the Bose-Hubbard model. However, the required cavity  $Q$  factor in this limit is about  $10^6$  to  $10^7$ , which is two to three orders of magnitude higher than the state of art in semiconductor cavity QED systems [13]. The ground state interaction energy  $U$  at large detuning is enhanced by increasing  $N$  due to the linear proportionality between optical Kerr nonlinearity and number of impurities [18]

$$\chi^{(3)} = \frac{2N |\mu_{eg}|^4}{3\epsilon_o \hbar^3 \Delta^3}. \quad (11)$$

$\mu_{eg}$  is the electric dipole moment matrix element. Such a trend is opposite to the case at near resonance shown in Fig. 3a. but can be understood by plotting  $U$  as a function of  $N$  and  $\Delta$  shown in Fig. 5. When the photons and excitons are coupled (small detuning limit), large  $N$  forces the system behaves linearly due to the boson-like collective angular momentum creation/annihilation operator. Dipole moments are vanishingly small at this limit and optical Kerr nonlinearity doesn't apply. However, when the photons and excitons are decoupled (large detuning limit), large  $N$  increases the total electric dipole moments so the optical Kerr nonlinearity seen by the photon-like branch of the cavity polaritons is enhanced.

Observing the QPT from a photonic superfluid to Mott-insulator requires the ability to control  $t$  and  $U$ . The frequency detuning can be used as such parameter. Varying a temperature can modulate the bound exciton transition frequency while keeping the cavity photon resonance frequency constant. Alternatively, injecting a molecular gas can modulate the cavity photon resonance frequency while keeping the bound exciton transition frequency constant. Signature of the QPT can be experimentally identified by observing the far field radiation just like in the optical lattice experiments [2]. Another

way to identify the QPT is to inject photons by end-firing the membrane layer and measure the transmission from the whole structure. High and low transmissions correspond to the superfluid and the Mott-insulator regimes, respectively.

In conclusion, we propose and investigate an experimental scheme to observe the photonic QPT. Our scheme is based on two recent experimental breakthroughs, highly homogeneous substitutional donor/acceptor impurities in semiconductor, and photonic crystal microcavities with high cavity  $Q$  factor and small mode volume. The QPT condition is robust against the fluctuation of number of impurities, and only a moderate cavity  $Q$  factor is required when using a large blue detuning. We also show that the many-exciton cavity QED Hamiltonian is reduced to the conventional Bose-Hubbard model for the ground state in the large red detuning limit. Finally, we point out that due to the flexibility of designing microcavity array topology, systems such as extended Bose-Hubbard model [19] or one-dimension Tonks-Girardeau gas [20] could also be simulated by our scheme.

Y.C. Neil Na is partially supported by MediaTek Fellowship. We would like to thank Patrik Recher, Kai-Mei Fu, Tim Byrnes, George Roumpos, Chih-Wei Lai, Sougato Bose and Andrew Greentree for useful discussions. This work is partially supported by SORST program of Japan Science of Technology Corporation (JST) and NTT Basic Research Laboratories.

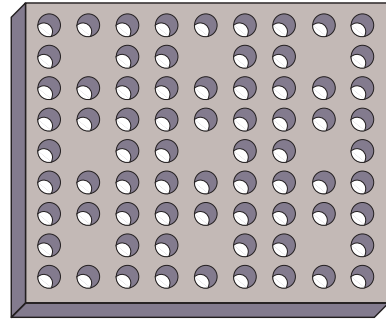


**FIG. 1. Schematic plot for a two-dimensional array of photonic crystal microcavities.**

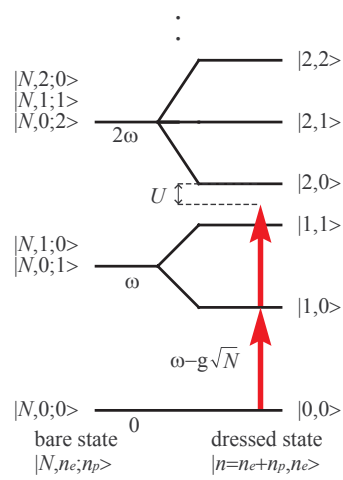


**FIG. 2. The eigenenergy spectrum of a many-exciton cavity QED system at zero frequency detuning.  $N \geq 2$  is assumed. The ground state interaction energy  $U$  for adding a subsequent photon to the cavity is labeled.**

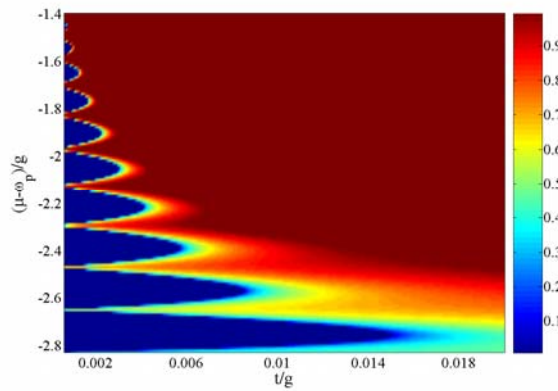


**FIG. 3.** Zero-temperature phase diagram obtained by plotting the superfluid parameter as a function of  $t$  and  $\mu$ .  $N=8$  and  $\Delta=0$  are assumed. The lowest Mott lobe corresponds to one photon per cavity; the second lowest Mott lobe corresponds to two photons per cavity and so forth.

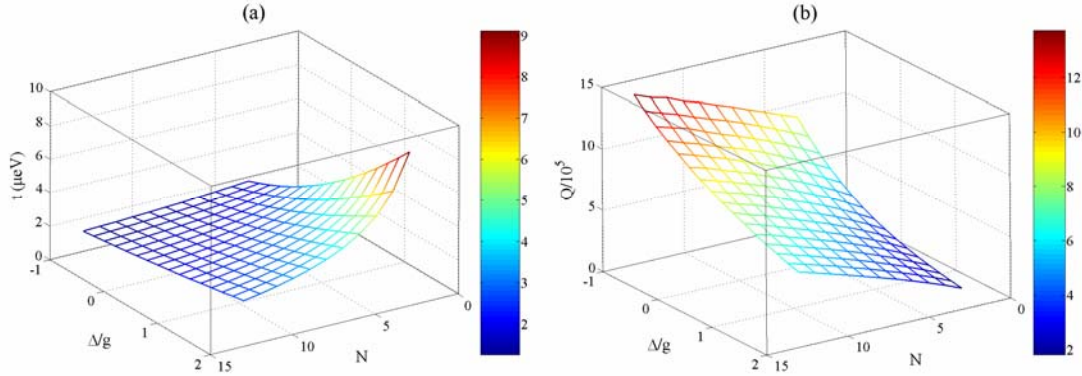


**FIG. 4.** The required (a) tunneling energy and (b) cavity  $Q$  factor for the system to enter the Mott-insulator regime with one photon per cavity as a function of  $N$  and  $\Delta$ .

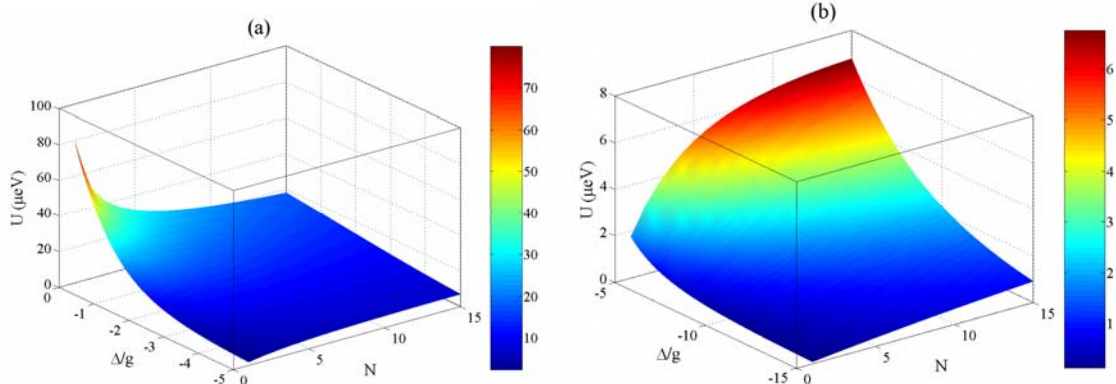


**FIG. 5.** The ground state interaction energy  $U$  plotted as a function of  $N$  and  $\Delta$  in (a) the small red detuning limit and (b) the large red detuning limit.

- [1] R. P. Feynman, *Int. J. Theor. Phys.* **21**, 467 (1982).
- [2] M. Greiner, O. Mandel, T. Esslinger, T. W. Hänsch and I. Bloch, *Nature* **415**, 39 (2002).
- [3] M. Köhl, H. Moritz, T. Stöferle, K. Günter and T. Esslinger, *Phys. Rev. Lett.* **94**, 080403 (2005).
- [4] D. Jaksch, C. Bruder, J. I. Cirac, C. W. Gardiner and P. Zoller, [4] D. Jaksch and P. Zoller, *Annals of Physics* **315**, 52 (2005).
- [5] M. J. Hartmann, F. G. S. L. Brandão and M. B. Plenio, *Nature Phys.* **2**, 849 (2006).
- [6] D. G. Angelakis, M. F. Santos and S. Bose, Preprint at <<http://arxiv.org/abs/quant-ph/0606159>> (2006).
- [7] A. D. Greentree, C. Tahan, J. H. Cole and L. C. L. Hollenberg, *Nature Phys.* **2**, 856 (2006).
- [8] A. Imamoglu, H. Schmidt, G. Woods and M. Deutsch, *Phys. Rev. Lett.* **79**, 1467 (1997).
- [9] K. M. Birnbaum, A. Boca, R. Miller, A. D. Boozer, T. E. Northup and H. J. Kimble, *Nature* **436**, 87 (2005).
- [10] H. Altug and J. Vučković, *Appl. Phys. Lett.* **84**, 161 (2004).
- [11] C. J. Hwang, *Phys. Rev. B* **8**, 646 (1973).
- [12] K. C. Fu, C. Santori, C. Stanley, M. C. Holland and Y. Yamamoto, *Phys. Rev. Lett.* **95**, 187405 (2005).
- [13] T. Yoshie, A. Scherer, J. Hendrickson, G. Khitrova, H. M. Gibbs, G. Rupper, C. Ell, O. B. Shchekin and D. G. Deppe, *Nature* **432**, 200 (2004).

[14] K. Sheshadri, H. R. Krishnamurthy, R. Pandit and T. V. Ramakrishnan, *Europhys. Lett.* **22**, 257 (1993).

[15] Y. Yamamoto and A. Imamoglu, *Mesoscopic Quantum Optics* (Johns Wiley & Sons, 1999).

[16] M. Fujita, S. Takahashi, Y. Tanaka, T. Asano and S. Noda, *Science* **308**, 1296 (2005).

[17] D. Englund, D. Fattal, E. Waks, G. Solomon, B. Zhang, T. Nakaoka, Y. Arakawa, Y. Yamamoto and J. Vučković, *Phys. Rev. Lett.* **95**, 013904 (2005).

[18] Boyd, *Nonlinear Optics* (Academic Press, 2003).

[19] V. W. Scarola and S. Das Sarma, *Phys. Rev. Lett.* **95**, 033003 (2005).

[20] E. H. Lieb and W. Liniger, *Phys. Rev.* **130**, 1605 (1963).